(Received 14 February 2024, Accepted 25 March 2024, Scheduled 3 April 2024)

A Simplified Extended Multilayer SIW Supporting TE_{01} Mode Integrated with a Feeding Structure

Tzichat M. Empliouk[1], Christos I. Kolitsidas[2], and George A. Kyriacou[1,*]

[1]*Department of Electrical and Computer Engineering, Democritus University of Thrace, Xanthi, GR67100, Greece*
[2]*Ericsson, Standards & Technology — HW Research, Kista 164 80, Sweden*

ABSTRACT: In this letter, a TE_{01} operation of a multilayered Substrate Integrated Waveguide (SIW) is presented. To enable the propagation of this typically unsupported mode, the SIW is integrated with feeding layer and with an Electromagnetic Band Gap (EBG) structure, exciting and confining the field within the proposed waveguide structure. The EBG is simply stacked on top and bottom of the proposed structure, allowing for ease of manufacturing. The overall proposed structure is simulated and measured, and the results indicate very low insertion loss in the passband of the waveguide.

1. INTRODUCTION

There has been very active research on substrate integrated waveguide solutions in recent years due to their manufacturing simplicity in printed circuit board (PCB) technology and low losses. Their applications span waveguiding structures [1], antennas [2], microwave circuits including power dividers [3, 4], baluns [5, 6], and filters [7]. There are also efforts to integrate them with electronics [8, 9] for lower losses at higher frequencies. The standard SIW waveguide typically supports TE_{10} mode, with its application in microwave and RF systems as an antenna launcher offering a single linear polarization.

In order to exploit the benefits of polarization diversity (e.g., increased capacity) several topologies and feeding structures which support TE_{01} mode have been proposed in the past years. In [10], a single layered SIW is used to support the propagation of TE_{01} mode. This is achieved creating an air hole pattern nonradiative dielectric (NRD) guide by placing regions with lower dielectric constant outside the SIW in order to minimize the radiation losses. The NRD configuration of air holes is also used in [11, 12] with the combination of microstrip lines and tapered slotlines for the excitation of the TE_{01} mode. Recently, in [13] a single SIW with groove arrays combined with microstrip-to-slot line feeding was proposed as another planar configuration for excitation of the TE_{01} mode. The drawback of the aforementioned configurations is the excitation of higher-order mode (e.g., TE_{02}). Multilayered SIW structures acting as 180° polarizers are used in [14, 15] for the excitation of TE_{01} mode. These configurations are comprised of two stacked SIWs, sharing a common ground plane with tapered slot in [14] and with a stepped slot cut in [15]. However, these structures require a coupler and phase shifter in order to work as 180° polarizer.

In this work, we propose a new topology for the excitation of the TE_{01} mode based on a multilayer SIW arrangement integrated with microstrip to slot transition as a feeding excitation. The novel contribution herein with respect to [10–13], is that the whole topology is integrated with an EBG structure, which suppress the propagation of undesired modes and minimize the radiation losses outside the SIW waveguide. Moreover the structure resembles a transmission line and does not require additional components like in [14, 15], offering simplicity and ease manufacturing.

This letter is organized as follows. Section 2 provides a detailed description of the proposed topology, while Section 3 presents the constructed prototype along with its simulated and measured results. Finally in Section 4, some conclusions are drawn for the proposed work.

2. PROPOSED WAVEGUIDING STRUCTURE

The proposed waveguide with the integrated feeding structure is illustrated in Fig. 1(a). The feeding structure is implemented with a simple microstrip to slotline transition ending with a linear taper in the waveguide similar to [11, 12]. The overall stack-up of the materials is depicted in Fig. 1(b) where the microstrip to slotline transition layer (feeding layer) is inserted between the top and bottom SIWs. In this manner, a double SIW (dSIW) is formed which shares the common slotted ground plane of the feeding layer. Fig. 1(b) also illustrates the top and bottom EBG structures which do not necessitate bonding materials, and they can be mechanically fastened. This simplifies the overall construction and costs as it avoids blind vias.

Figure 2(a) depicts the unit cell of the proposed dSIW configuration. It is composed of two SIWs positioned in a back-to-back arrangement, with the feeding layer embedded between the two SIWs. Metallised vias with 0.7 mm diameter and a period spacing of 0.91 mm are used as side walls as shown in Fig. 2(a). An eigen-analysis of the unit cell is performed first, in order to identify the possible propagating modes, their es-

* Corresponding author: George A. Kyriacou (gkyriac@ee.duth.gr).

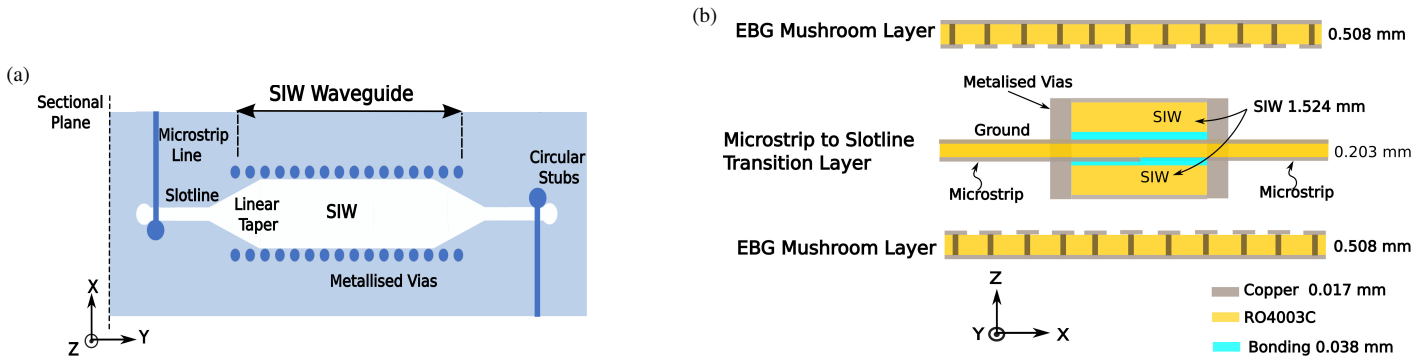

FIGURE 1. (a) The proposed waveguide topology. (b) Side view and material stack-up for the proposed waveguide.

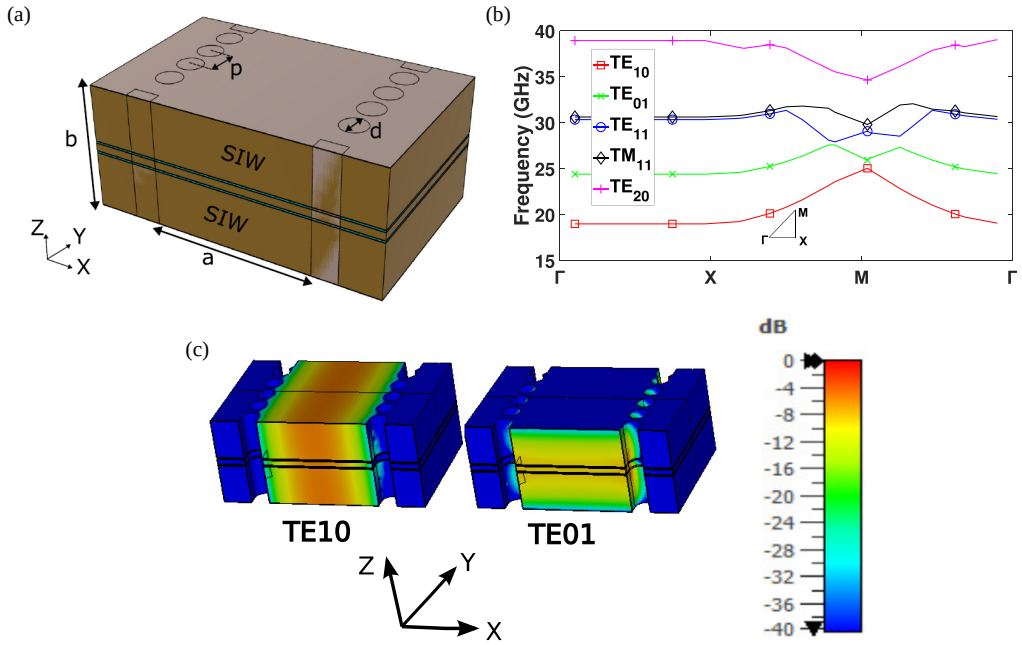

FIGURE 2. (a) dSIW unit cell with $a = 4.3$, $b = 3.429$, $d = 0.7$ and $p = 0.91$ (Dimensions are in mm). (b) Dispersion diagram for the first five modes of the dSIW unit cell. (c) Electric field distribution for the TE_{10} and TE_{01} modes.

sential field components along with their modal field distribution. The resulting dispersion diagram for the first five modes is illustrated in Fig. 2(b). Fig. 2(c) depicts the electric field distributions of the first two modes, TE_{10} and TE_{01} modes. As expected, the dominant mode is TE_{10} mode with strong vertical transverse E_z component (the propagation direction is y) and a cut-off frequency at 19 GHz. However, a TE_{01} mode with a dominant E_x component is also supported with a cut-off frequency at 24.3 GHz as depicted again in Figs. 2(b) and 2(c). The purpose of this work is to excite the TE_{01} mode while suppressing any other mode. This is achieved in two steps. In the first step, a feeding structure is employed, providing a strong E_x component but negligible E_z thus avoiding any energy coupling to the dominant (lower cut-off) TE_{10} mode. This is indeed possible by utilizing the tapered slotline of Fig. 1(a) since its dominant field is normal to slot walls. An ordinary slotline with characteristic impedance of $Z_{0s} \approx 100\,\Omega$ is considered, which is fed by a transversely placed microstrip line with $Z_{0m} = 50\,\Omega$. Both the microstrip and slotline are terminated to circular stubs to ensure wideband matching [16]. In turn, the slotline is tapered, increasing its aperture to match the SIW characteristic impedance. In the second step, an EBG in the form of a periodic structure is utilized to avoid the propagation of undesired modes in the feeding layer. The EBG structure described next is commonly employed in Gap waveguide technologies. Hence, to the best of authors' knowledge it is the first time that it is integrated with a SIW structure.

The proposed EBG unit cell, depicted in Fig. 3(a), is the classic mushroom type [17]. It consists of a rectangular patch of width w_m connected to ground through a metallised via of diameter d_v. Rogers RO4003C with $\epsilon_r = 3.38$ and height of h_{sm} is used as a dielectric substrate. The spacing of adjacent unit cells is denoted as s as shown in Fig. 3(a). This EBG structure behaves as a network of parallel resonant LC circuit with the resonance frequency given from the relation:

$$\omega_0 = 1/\sqrt{LC} \tag{1}$$

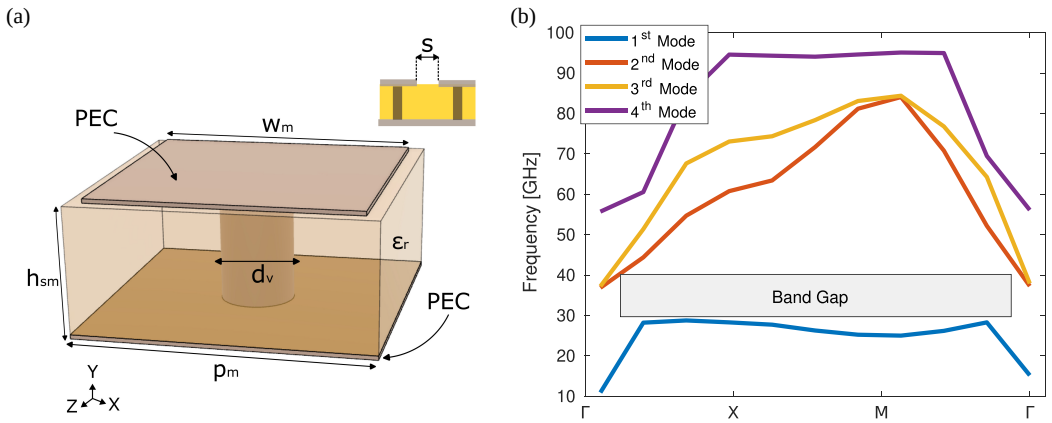

FIGURE 3. (a) The designed EBG unit cell. $p_m = 1.2$, $h_{sm} = 0.508$, $w_m = 1.08$, $d_v = 0.3$ and $s = 0.12$ (Dimensions are in mm). (b) Dispersion diagram and of the EBG unit cell.

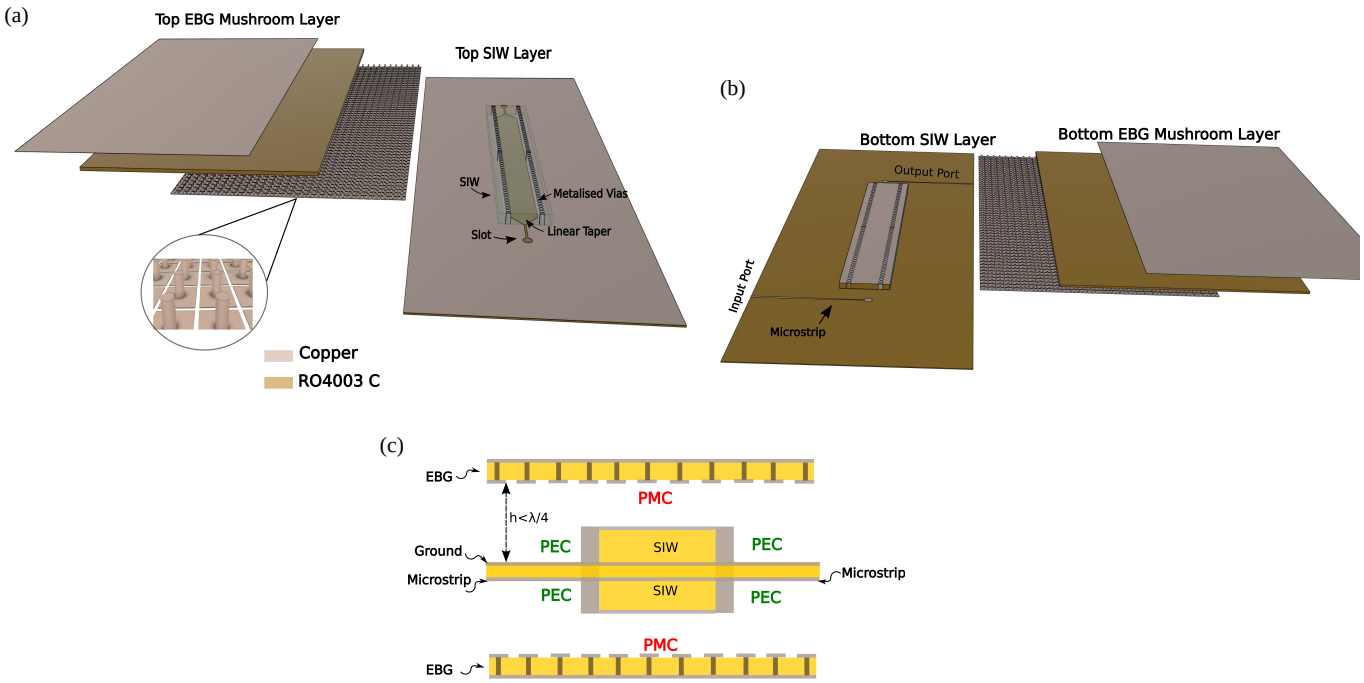

FIGURE 4. The proposed waveguide topology. (a) Top view. (b) Bottom view. (c) PMC-PEC condition utilization between the layers.

At the resonance, the EBG structure creates a bandgap region in which it exhibits a high surface impedance, suppressing surface waves of either polarization [17]. Since the EBG structure behaves as an artificial magnetic conductor (AMC), it creates a parallel plate's stopband when being integrated with a microstrip line, as in our case. This means that it stops the propagation of field in any direction except along the microstrip [18]. Consequently, the desired bandgap as well as the related bandwidth of the EBG is defined totally by its geometrical characteristics. Referring to Fig. 3(a), the parameters w_m, h_{sm}, d_v, and s are tuned in order to achieve the desired bandgap. The resulting dispersion diagram is shown in Fig. 3(b) where a bandgap region from 30 to 40 GHz with a centre frequency of 35 GHz was attained in the waveguide propagating band.

3. WAVEGUIDE RESULTS

Once the feeding structure, waveguide transition, dSIW, and EBG are separately designed and optimized, they are integrated yielding the overall proposed waveguide in a back to back configuration as illustrated in Fig. 4. Therein the exploded view is shown to clarify the representation of the different layers. In Fig. 4(a), the top SIW is presented in a transparent view in order to show the linear taper and slotted ground where the coupling between the two SIWs occurs. Input and output microstrip ports are located in bottom SIW layer as shown Fig. 4(b). Fig. 4(c) depicts the perfect magnetic conductor (PMC)-perfect electric conductor (PEC) condition formed by the EBG layers and feeding layer. As noted earlier, the EBG structure behaves as a PMC, and as long as the distance between the EBG and the feed-

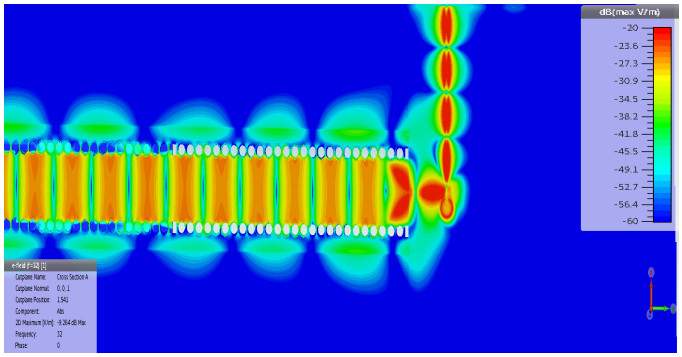

FIGURE 5. Electric field distribution at the longitudinal cross section of the waveguide.

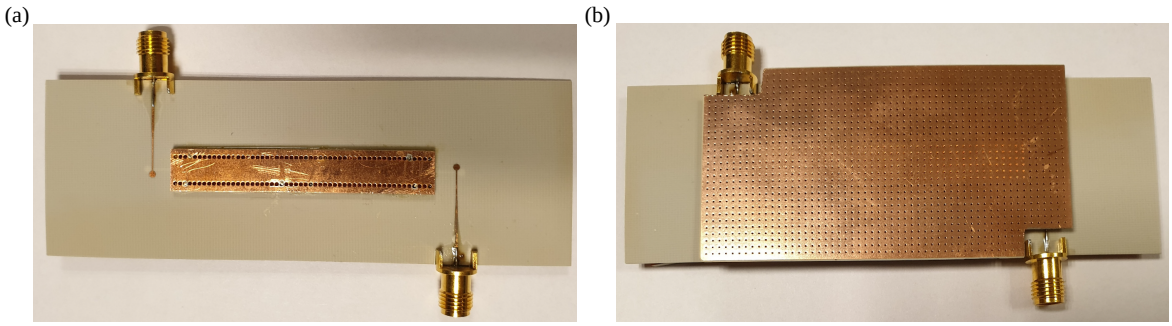

FIGURE 6. Constructed waveguide structure, (a) feeding structure and dSIW only and (b) after fastening the EBG layer to the dSIW.

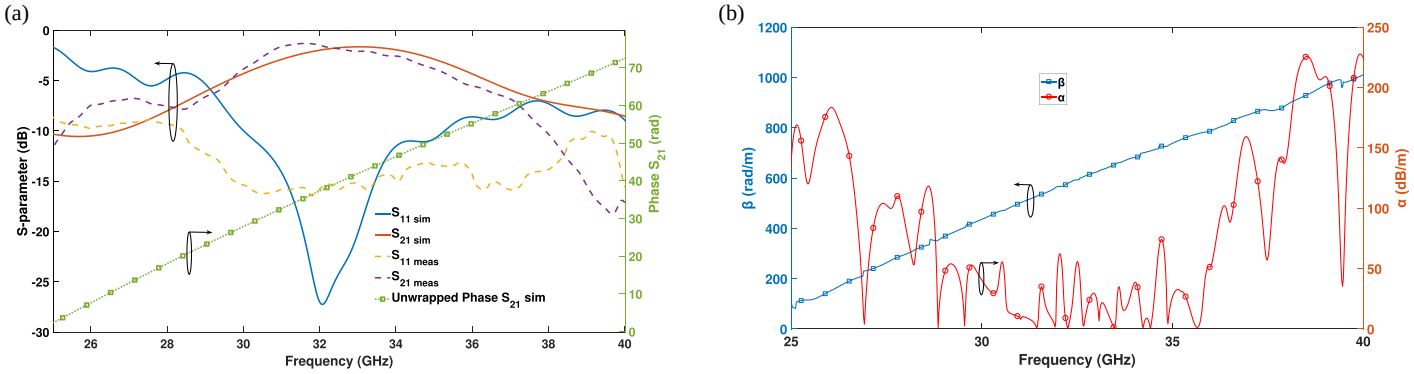

FIGURE 7. (a) Simulated and measured S-parameter results for the entire structure. (b) Simulated phase and attenuation constants for the dSIW.

ing layer is less than quarter wavelength, no propagating modes occur in any direction between these layers. The only allowed mode is the local mode between microstrip and ground (PEC-PEC) which is the quasi-TEM mode, just like in microstrip GAP waveguides [19]. The quasi-TEM mode is then converted to TE_{01} mode via the linear taper slot.

The field confinement is depicted in Fig. 5 where the benefits of the proposed configuration are clearly shown since the TE_{01} mode is successfully excited, and the field is confined within the double SIW topology. Furthermore, as depicted in Fig. 5 the field outside the walls of the dSIWs is significantly reduced, minimizing radiation losses due to the presence of the PMC-PEC condition outside the dSIWs. The proposed structure is fabricated as shown in Fig. 6 and measured using a vector network analyzer. The simulated and measured transmission and reflection S-parameters for port 1 are depicted in Fig. 7(a). It is worth mentioning that in the mid of the pass-band, the overall loss of the entire structure is approximately 1.5 dB where only the length of the dSIW is 50 mm. Fig. 7(b) depicts the phase constant β (left) and attenuation constant α (right) of the de-embedded dSIW. The de-embedding process aims at the extraction of the S-parameters of the dSIW only (including the linear taper sections). Thus, the feeding structure is separately designed as a two-port network and simulated to obtain its S-parameters. Subsequently, the S-parameters of the whole structure and that of the feeding structure are imported in a Keysight ADS de-embedding scheme in order to extract the S-parameters of the dSIW only. Finally, utilizing the extracted S-parameters, the phase and attenuation constants are calculated using the relationships outlined in [20]. Upon exam-

ination of the simulated magnitude and the unwrapped phase of the S_{21} parameter in Fig. 7(a) alongside Fig. 7(b), a good agreement is observed with the corresponding phase and attenuation constant curves.

4. CONCLUSION

In this work, a multilayered dSIW integrated, with a feeding layer and an EBG structure, is proposed and successfully designed and fabricated. A mushroom type EBG was employed to suppress the propagation of undesired modes allowing only the propagation of TE_{01} mode. Manufacturing simplicity is achieved by simply stacking the EBG structures on top and bottom. The overall fabricated structure is measured, and the results indicate very low insertion loss in the passband of the waveguide.

ACKNOWLEDGEMENT

The authors would like to thank Dr. Lei Wang for the significant contribution in the development of the concept.

REFERENCES

[1] Esparza, N., P. Alcón, L. F. Herrán, and F. Las-Heras, "Substrate integrated waveguides structures using frequency selective surfaces operating in stop-band (SBFSS-SIW)," *IEEE Microwave and Wireless Components Letters*, Vol. 26, No. 2, 113–115, Feb. 2016.

[2] Bharath, K., S. V. Nandigama, D. Ramakrishna, and V. M. Pandharipande, "High performance millimeter wave SIW slotted array antenna," *Progress In Electromagnetics Research C*, Vol. 125, 15–23, 2022.

[3] He, Z., J. Cai, Z. Shao, X. Li, and Y. Huang, "A novel power divider integrated with SIW and DGS technology," *Progress In Electromagnetics Research*, Vol. 139, 289–301, 2013.

[4] Chen, Z., D. Guan, Z. Qian, and W. Wu, "Dual-mode power divider and its application in monopulse antenna," *IEEE Transactions on Circuits and Systems II: Express Briefs*, Vol. 69, No. 12, 4839–4843, 2022.

[5] Zhang, T., L. Li, Z. Zhu, and T. J. Cui, "A broadband planar balun using aperture-coupled microstrip-to-SIW transition," *IEEE Microwave and Wireless Components Letters*, Vol. 29, No. 8, 532–534, Aug. 2019.

[6] Jia, M., J. Zhang, and Y. Dong, "A compact and broadband balun based on multilayer SIW," *IEEE Microwave and Wireless Components Letters*, Vol. 32, No. 2, 105–108, 2022.

[7] Wu, Y., Y. Yu, P. Su, X. Zhang, L. Wang, and S. Wang, "Design of compact SIW bandpass filter with high selectivity," *Progress In Electromagnetics Research Letters*, Vol. 112, 35–40, 2023.

[8] Roev, A., R. Maaskant, A. Höök, and M. Ivashina, "Wideband mm-Wave transition between a coupled microstrip line array and SIW for high-power generation MMICs," *IEEE Microwave and Wireless Components Letters*, Vol. 28, No. 10, 867–869, Oct. 2018.

[9] Roev, A., J. Qureshi, M. Geurts, R. Maaskant, M. K. Matters-Kammerer, and M. Ivashina, "A wideband mm-Wave Watt-level spatial power-combined power amplifier with 26on Microwave Theory and Techniques, Vol. 70, No. 10, 4436–4448, 2022.

[10] Cassivi, Y. and K. Wu, "Substrate integrated circuits concept applied to the nonradiative dielectric guide," *IEE Proceedings — Microwaves, Antennas and Propagation*, Vol. 152, No. 6, 424–433, Dec. 2005.

[11] Esquius-Morote, M., B. Fuchs, J.-F. Zürcher, and J. R. Mosig, "Extended SIW for TE_{m0} and TE_{0n} modes and slotline excitation of the TE_{01} mode," *IEEE Microwave and Wireless Components Letters*, Vol. 23, No. 8, 412–414, Aug. 2013.

[12] Esquius-Morote, M., M. Mattes, and J. R. Mosig, "Orthomode transducer and dual-polarized horn antenna in substrate integrated technology," *IEEE Transactions on Antennas and Propagation*, Vol. 62, No. 10, 4935–4944, 2014.

[13] Chen, Z., D. Guan, Z. Qian, and W. Wu, "Dual-polarized SIW leaky-wave antenna based on mode-multiplexed feeding structure," *IEEE Antennas and Wireless Propagation Letters*, Vol. 22, No. 1, 104–108, 2023.

[14] Li, A. and K.-M. Luk, "Millimeter-wave dual linearly polarized endfire antenna fed by 180° hybrid coupler," *IEEE Antennas and Wireless Propagation Letters*, Vol. 18, No. 7, 1390–1394, 2019.

[15] Xia, X., F. Wu, C. Yu, Z. H. Jiang, R. Lu, Y. Yao, and W. Hong, "Millimeter-wave ±45° dual linearly polarized end-fire phased array antenna for 5G/B5G mobile terminals," *IEEE Transactions on Antennas and Propagation*, Vol. 70, No. 11, 10 391–10 404, 2022.

[16] Knorr, J. B., "Slot-line transitions (short papers)," *IEEE Transactions on Microwave Theory and Techniques*, Vol. 22, No. 5, 548–554, 1974.

[17] Sievenpiper, D., L. Zhang, R. F. J. Broas, N. G. Alexopolous, and E. Yablonovitch, "High-impedance electromagnetic surfaces with a forbidden frequency band," *IEEE Transactions on Microwave Theory and Techniques*, Vol. 47, No. 11, 2059–2074, 1999.

[18] Pucci, E., E. Rajo-Iglesias, and P.-S. Kildal, "New microstrip gap waveguide on mushroom-type EBG for packaging of microwave components," *IEEE Microwave and Wireless Components Letters*, Vol. 22, No. 3, 129–131, 2012.

[19] Rajo-Iglesias, E., A. U. Zaman, and P.-S. Kildal, "Parallel plate cavity mode suppression in microstrip circuit packages using a lid of nails," *IEEE Microwave and Wireless Components Letters*, Vol. 20, No. 1, 31–33, 2010.

[20] Eisenstadt, W. R. and Y. Eo, "S-parameter-based IC interconnect transmission line characterization," *IEEE Transactions on Components, Hybrids, and Manufacturing Technology*, Vol. 15, No. 4, 483–490, 1992.